frontiers | Frontiers in Earth Science

TYPE Original Research
PUBLISHED 17 January 2023
DOI 10.3389/feart.2022.1020594

Check for updates

OPEN ACCESS

EDITED BY
Hermínio Araújo-Júnior,
Rio de Janeiro State University, Brazil

REVIEWED BY
Ismar De Souza Carvalho,
Federal University of Rio de Janeiro, Brazil
Kamila Bandeira,
Federal University of Rio de Janeiro, Brazil
Fernando Barbosa,
Rio de Janeiro State University, Brazil

*CORRESPONDENCE
Yan Zhao,
zhaoyan@lyu.edu.cn

SPECIALTY SECTION
This article was submitted to Paleontology, a section of the journal Frontiers in Earth Science

RECEIVED 18 August 2022
ACCEPTED 25 November 2022
PUBLISHED 17 January 2023

CITATION
Zhao Y, Tian Q, Ren G-Y, Guo Y and Zheng X-T (2023), Taphonomic analysis of the exceptional preservation of early bird feathers during the early Cretaceous period in Northeast China. *Front. Earth Sci.* 10:1020594. doi: 10.3389/feart.2022.1020594

COPYRIGHT
© 2023 Zhao, Tian, Ren, Guo and Zheng. This is an open-access article distributed under the terms of the Creative Commons Attribution License (CC BY). The use, distribution or reproduction in other forums is permitted, provided the original author(s) and the copyright owner(s) are credited and that the original publication in this journal is cited, in accordance with accepted academic practice. No use, distribution or reproduction is permitted which does not comply with these terms.

Taphonomic analysis of the exceptional preservation of early bird feathers during the early Cretaceous period in Northeast China

Yan Zhao[1]*, Qian Tian[2], Guang-Ying Ren[1], Ying Guo[1] and Xiao-Ting Zheng[1,3]

[1]Institute of Geology and Paleontology, Linyi University, Linyi, China, [2]School of Life Sciences, Yan'an University, Yan'an, China, [3]Shandong Tianyu Museum of Nature, Linyi, China

Fossil soft tissues contain important and irreplaceable information on life evolution, and on the comprehensive understanding of the nature of Mesozoic ecosystems. Compared to other fossil soft tissues, Jehol Biota feathers are more commonly reported. However, taphonomic analysis of these feathers is lacking. Here, five Jehol Biota specimens of early bird *Sapeornis chaoyangensis* with differently preserved feathers were selected. One specimen, STM 15-36, has a complete set of extraordinarily preserved feathers. An interesting consequence was revealed by their host sediment Zr/Rb analysis that specimen STM 15-36 possesses the coarsest sediment grain size but the best-preserved feathers. More geochemical analyses of host sediments, including organic carbon isotopes and major elements, were conducted to restore the paleoenvironment during those *Sapeornis*' burial. The result mainly shows that the paleoclimate when *Sapeornis* STM 15-36 was buried is warmer and wetter than those of the other four; STM 15-36 host sediment has a pure terrestrial-derived organic input, while the others are aquatic algae. In addition, redox-sensitive trace elements analysis indicates the lake bottom-water preserved *Sapeornis* STM 15-36 is anoxic and restricted, being more oxygen-depleted than those of the other four. Therefore, the transportation and burial of *Sapeornis* STM 15-36 were preliminarily inferred as: the carcass of *Sapeornis* STM 15-36 was transported rapidly into the lake by a short and strong rain flush, and then was buried quickly by the accompanying terrestrial debris; the subsequent anoxic and restricted burial environment inhibited bioturbation and hydrodynamic disturbance on *Sapeornis* STM 15-36 and its host sediments, allowing its whole set of feathers to be delicately preserved. This finding provides a valuable case study on understanding the taphonomy of fossil soft tissues' exceptional preservation in Jehol Biota.

KEYWORDS

fossil preservation, feathers, early bird, Cretaceous, Jehol Biota

Introduction

The Jehol Biota, one of the most important Mesozoic fossil Lagerstätten, comprises extraordinary taxonomic diversity of micro- and megaplants, invertebrates, and vertebrates; moreover, it provides the most informative source for understanding Mesozoic ecology (Chang et al., 2003; Wang and Zhou, 2003; Zhou et al., 2003; Jiang et al., 2011; Pan et al., 2012; Carvalho et al., 2015a; Carvalho et al., 2015b). An exceptionally set of well-preserved soft tissues are reported for myriad taxa, especially internal organs and dermal appendices (including feathers and furs) of early birds, feathered dinosaurs, and primitive mammals, which contain most important and irreplaceable information for understanding the early evolution of biological and ecological characteristics (Zhang and Zhou, 2004; Zhang et al., 2010; Pan et al., 2016; Wang et al., 2017a; Wang et al., 2018; McNamara et al., 2018; Pan et al., 2019; Serrano et al., 2020; Ullmann et al., 2020; Cincotta et al., 2022). For example, the reported specimens of basal birds with feathers, including the *Jeholornis*, confuciusornithidormes, and *Enantiornithes* present the morphology, arrangement, and even three-dimensional structure of early feathers (Chuong et al., 2003; Zhang and Zhou, 2004; Zhang et al., 2006; Foth, 2012; O'Connor et al., 2012; Wang et al., 2014; Carvalho et al., 2015a). This information currently constitutes the most knowledge of the early evolution of bird feathers and flight. Different preservations of fossil soft tissues are present in the biota (Zhou, 2014). However, taphonomic-related studies mainly demonstrated that soft tissue preservation is linked to the deposition of finely laminated sediments (shales or mudstones), which are interbedded with ash layers (Zhou, 2014; Xu et al., 2019), and volcanic eruptions (Wang et al., 1999; Guo and Wang, 2002; Guo et al., 2003; Jiang and Sha, 2007; Jiang et al., 2011; Jiang et al., 2012; Pan et al., 2012; Pan et al., 2013a; Jiang et al., 2014; Xu et al., 2019). More details concerning the taphonomy of different preserved fossil soft tissues are lacking, but this information is essential for comprehensively understanding the taphonomy of the Jehol Biota and for the overall recovery of Mesozoic ecology.

In particular, taphonomic analysis of the preservation of the same fossil soft tissues is still lacking. Compared to other fossil soft tissues, e.g., lungs (Wang et al., 2018) and ovarian follicles (Wang et al., 2016; Zheng et al., 2017), fossil feathers are more commonly reported among early birds and feathered dinosaurs of the Jehol Biota; these feathers usually present various manners of preservation from fuzzy imprints to delicate morphology and structures. Therefore, specimens containing differently preserved feathers could provide ideal materials to probe the taphonomic effects on fossil soft tissues' exceptional preservation. *S. chaoyangensis* is one of the basal birds, being distinctive in its elongated wings, large body size, and absence of ossified sternum (Zhou and Zhang, 2002; Zhou and Zhang, 2003; Zheng et al., 2014). In this study, five specimens with various states of feather preservation were selected from two excavation regions in Western Liaoning. One specimen (STM 15-36), in particular, has extraordinarily preserved feathers of the complete set (Zheng, 2009). Then, the paleoenvironment when each specimen was buried, and subsequent burial conditions were reconstructed by the geochemical analysis of the host sediments. The burial environment features of the exceptionally well-preserved specimen and others were compared to further probe how environmental settings influence the extraordinary preservation of feathers.

Geological setting

The western Liaoning area, where most of the typical Jehol Biota occurs, was located in the northeast part of the North China Craton in a terrestrial environment at a paleolatitude of approximately 40–45°N during the late Mesozoic (Figures 1A,B; Zhou et al., 2003). In the Early Cretaceous, a series of basins were formed in western Liaoning due to increased tectonic and magmatic activity. The corresponding lacustrine sedimentary strata (Jehol Group; Gu, 1962) consist of the Yixian Formation, Jiufotang Formation, and Fuxin Formation from bottom to top (Sha, 2007). The Yixian Formation rests unconformably on the Tuchengzi Formation and is mainly composed of multiple eruptive volcanic rocks with sedimentary intercalations; the Jiufotang Formation conformably overlies the Yixian Formation and is composed mainly of tuffaceous shale, mudstone, and sandstone; and the Fuxin Formation rests conformably on the Jiufotang Formation and consists primarily of sandstones and conglomerates alternating with mudstones, sandy shales and coalbeds (Gu, 1982; Sha, 2007; Zhou et al., 2021). Radiometric and paleomagnetic dating of volcanic material shows that the Yixian Formation occupied an age of mainly the Barremian around the Barremian-Aptian transition (Zhu et al., 2001; Zhu and He, 2003; Sha, 2007; Yang et al., 2007; Zhu and He., 2007), and the Jiufotang Formation was the early Aptian (He et al., 2004); the age of the Fuxin Formation was also assigned to the Aptian according to their composition of the bivalves (Sha, 2007).

The Dapingfang (DPF) and Toudaoyingzi (TDYZ) towns are under the jurisdiction of Chaoyang and Jianchang city in western Liaoning, respectively (Figure 1C), and are approximately 65 km apart. The two towns are both famous for the delicate preserved and diverse fossils contained in the Jiufotang Formation (Zhou et al., 2021). Various preserved fossils of the same species were discovered in both regions. For example, the feathers of the basal bird *S. chaoyangensis* (Zhou and Zhang, 2003; Provini et al., 2009;

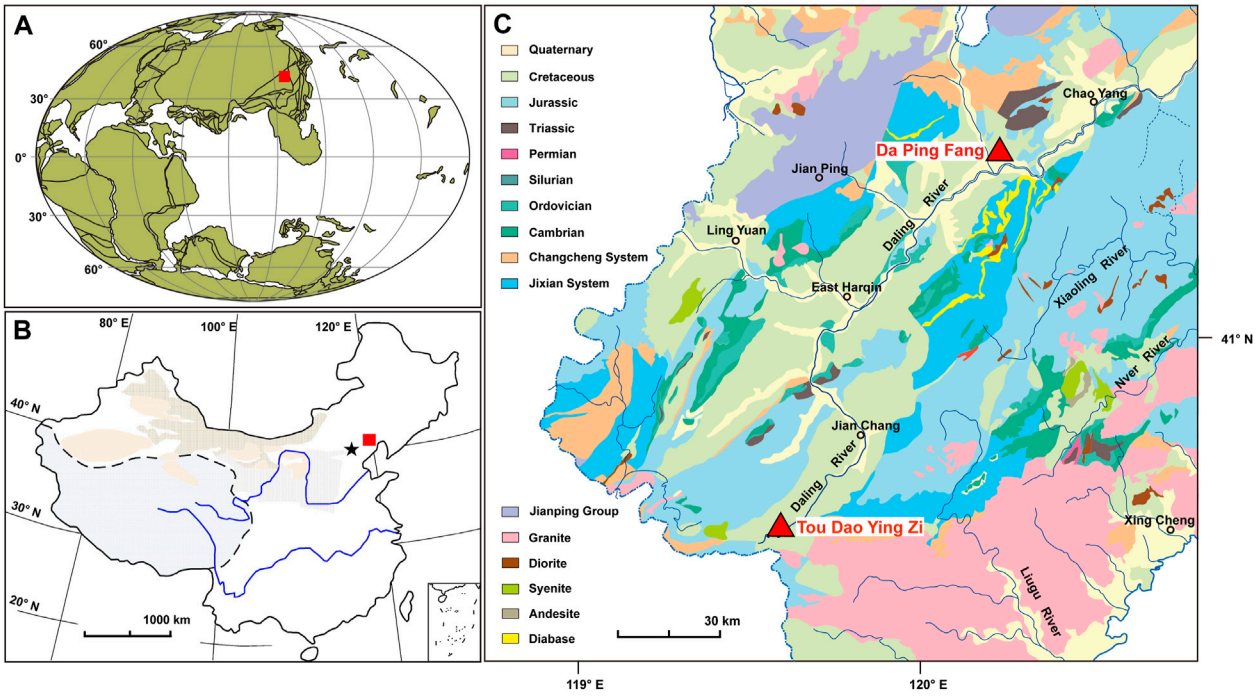

FIGURE 1
(A) Paleogeographic position (www.odsn.de) and **(B)** geographic position of the study area (red square); and **(C)** geological map of western Liaoning, China, and fossil sites in this study (red triangles).

Zheng, 2009; Wang et al., 2017b) from both DPF and TDYZ present different preservation, providing excellent material to investigate the paleoenvironmental effects on fossil (especially soft tissues) preservation.

Materials and methods

Five specimens of *S. chaoyangensis* with different preservation states on feathers (Figure 2; Table 1) were selected from the Shandong Tianyu Museum of Natural History (STM). All these specimens preserve a complete and articulated skeleton, indicating that decay was terminated at a stage before the skeleton became disarticulated (Pan et al., 2013a). The STM 15-36 feathers are best preserved among the five specimens and are even exquisite and rare in the reported *Sapeornis*. In addition, three host sediments from various sections of each specimen were also collected, and the three sediments are all from the same layer bearing the fossil.

The fifteen samples of sediment from *Sapeornis* specimens were ground in an agate mortar to a particle size of less than 150 μm. Approximately 2 g of the prepared samples were digested for 24 h in 2 mol•L^{-1} HCl at room temperature to remove carbonate and then washed with deionized water to pH >6 and dried at 60°C. The contents of total organic carbon (TOC) and nitrogen (TN) and the stable isotopic composition of organic carbon ($\delta^{13}C_{org}$) of the prepared samples were analyzed by an Isoprime 100-EA isotope mass spectrometer with precisions of < ±0.2‰. The $\delta^{13}C$ values of the samples are reported to the international standards of the Vienna Pee Dee Belemnite (VPDB). Besides, sediment C/N ratios are obtained by the atomic ratio of TOC and TN. The TOC, TN, and $\delta^{13}C$ analyses of samples were performed at the Institute of Environment and Sustainable Development in Agriculture, Chinese Academy of Agricultural Sciences, Beijing, China.

Furthermore, the ground samples were flattened to analyze the elemental characteristics of whole rocks by a handheld X-ray fluorescence Analyzer (Niton XL3t). The elemental contents above the detection limit are reported in parts per million (μg/g). Measured elements include Mn, Zr, Sr, Rb, Zn, Co, Fe, As, Nb, Mo, Cu, Ni, Pb, Th, U, and Ti. Sediment U/Th, Sr/Ca, Rb/Sr, and Zr/Rb ratios were also calculated by the ratio of related elements. This work was conducted at the Institute of Geology and Palaeontology, Linyi University.

Finally, statistical comparisons of the aforementioned indicators were conducted using Kruskal-Wallis analysis from the three groups, including STM 15-36 vs. STM 15-31 from TDYZ, STM 15-36 vs. three specimens from DPF, and two specimens from TDYZ vs. the three from DPF.

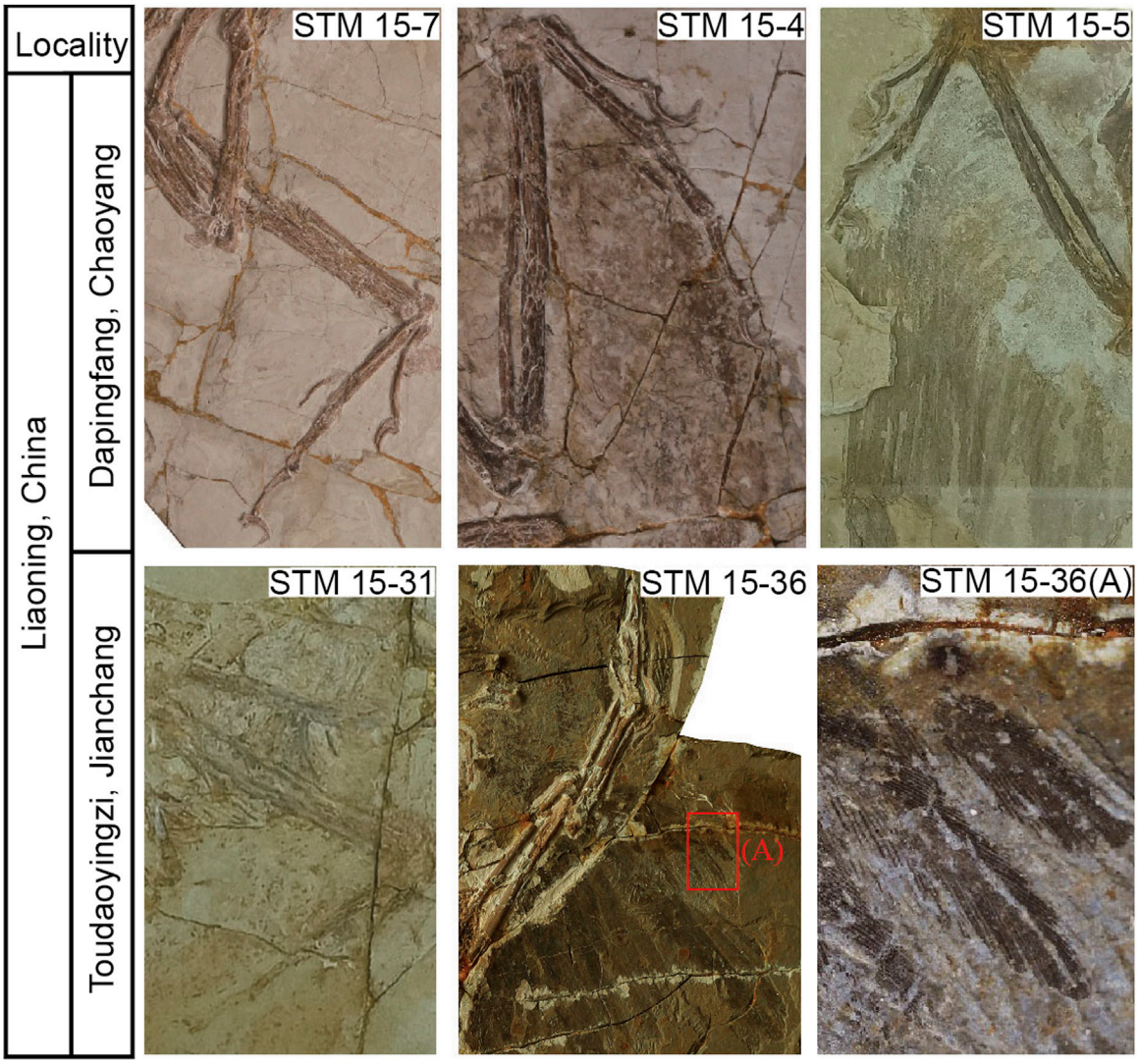

FIGURE 2
The forelimb feathers of *S. chaoyangensis* specimens present different preservations [STM 15-36(A) is the specific detail of forelimb feathers marked with a red rectangle (A) in STM 15-36].

TABLE 1 Feather preservations of the five *Sapeornis* specimens in this study.

Locality	Specimen	Feather preservation
Dapingfang	STM 15-7	Has no feathers
Dapingfang	STM 15-4	Only preserves weak imprints of wings
Dapingfang	STM 15-5	Only has clear wing imprints in which each feather fan can be distinguished
Toudaoyingzi	STM 15-31	Shows no evidence of feathers
Toudaoyingzi	STM 15-36	Preserves delicate and complete feathers, including information about ramus, vanes, and shafts

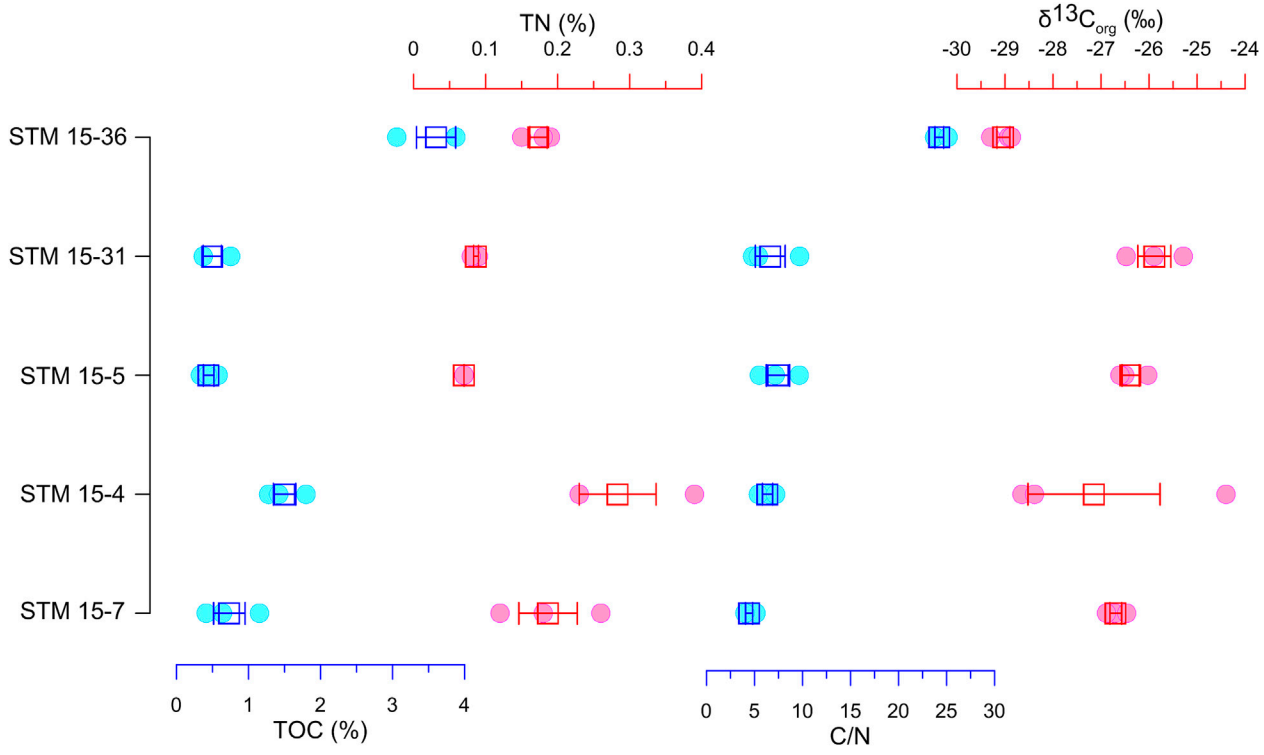

FIGURE 3
TOC, TN, C/N ratio, and $\delta^{13}C_{org}$ values of the host sediments of *Sapeornis* specimens.

Results

TOC, TN, C/N ratio, and $\delta^{13}C_{org}$ values of the host sediments

The TOC content of the host sediments from *Sapeornis* specimens distribute between 0.33% and 3.88%, with an average of 1.36% ± 1.26%. The sediment TN content range from 0.07% to 0.09%, and the mean value is 0.16% ± 0.09% (Figure 3). In addition, sediment C/N ratios were obtained by the molar ratio of TOC and TN, and they distribute between 3.99 and 25.15, with a mean value of 9.82 ± 7.66. The host sediment $\delta^{13}C_{org}$ values of those specimens range from −29.30‰ to −24.40‰, with the mean value being −27.03‰ ± 1.46‰.

Trace element characteristics of the host sediments

Generally, the element contents of the host sediment of specimen STM 15-36 are obviously higher than the corresponding indicators of the other four specimens. Trace elements such as Mo, Th, Ni, U, Ti, Co, Pb, and Cu in the sediments of specimens STM 15-31, STM 15-5, STM 15-4, and STM 15-7 are lower than the detected limit of the handheld X-ray fluorescence analyzer (Figure 4). Sediment Zr/Rb ratios are distributed between 1.54 and 2.41, with a mean value of 1.79 ± 0.27; sediment Rb/Sr ratios range from 0.28 to 0.54, with a mean value of 0.41 ± 0.08 (Table 2). In addition, the host sediment element indices of the other four specimens are standardized by the corresponding content of STM 15-36 (Figure 5). Except for the Sr and Mn contents of the STM 15-5 sediments, the other elemental contents and ratios are relatively deficient in the four specimens with relatively poor feather preservation.

Comparisons

Indicators that are suitable for effective Kruskal-Wallis analysis include TOC, TN, C/N, $\delta^{13}C_{org}$, Zr, Rb, Sr, Fe, As, Nb, Zn, Zr/Rb, and Rb/Sr (Table 3). For specimens from TDYZ, sediment TOC, TN, C/N ratios, and $\delta^{13}C_{org}$ values of STM 15-36 are significantly different from those of STM 15-31. For specimen STM 15-36 and the three specimens from DPF, only their sediment TN is comparable, whereas the others are significantly different. For the regional comparison, those sediment indicators between TDYZ and DPF show no

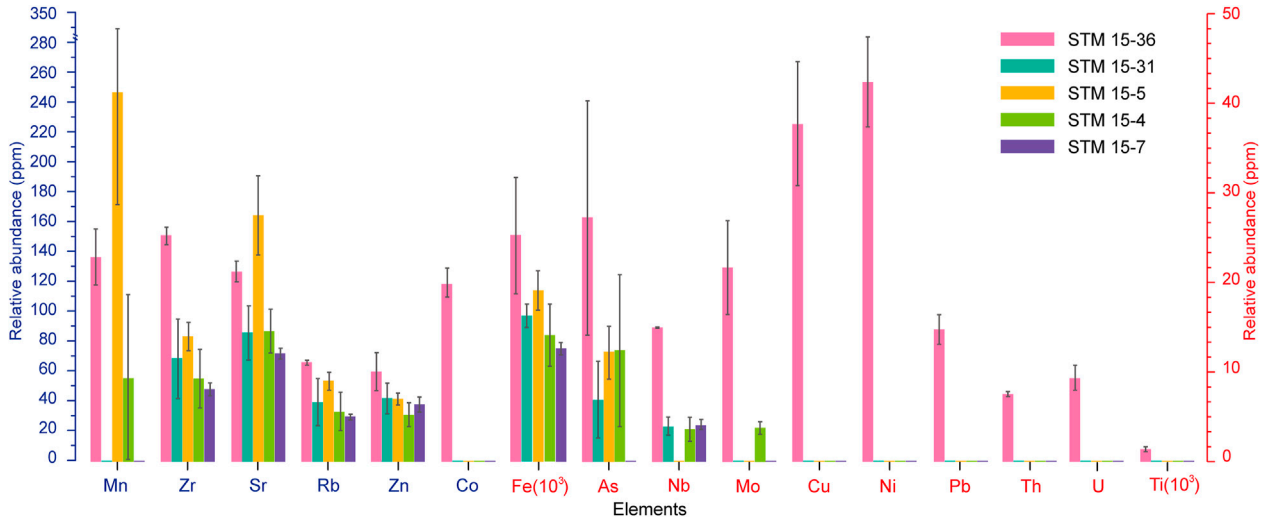

FIGURE 4
Element distribution of the host sediments from *Sapeornis* specimens.

TABLE 2 Indices derived from the elemental contents.

Samples		U/Th	Sr/Cu	Rb/Sr	Zr/Rb
STM 15-36	Sample 1	1.34	3.23	0.51	2.20
	Sample 2	1.40	3.05	0.51	2.41
	Sample 3	1.01	4.01	0.54	2.26
STM 15-31	Sample 1	-	-	0.37	1.84
	Sample 2	-	-	0.53	1.73
	Sample 3	-	-	0.44	1.70
STM 15-5	Sample 1	-	-	0.31	1.59
	Sample 2	-	-	0.35	1.55
	Sample 3	-	-	0.33	1.54
STM 15-4	Sample 1	-	-	0.38	1.69
	Sample 2	-	-	0.45	1.65
	Sample 3	-	-	0.28	1.79
STM 15-7	Sample 1	-	-	0.41	1.61
	Sample 2	-	-	0.42	1.68
	Sample 3	-	-	0.39	1.62

"-" indicates no data.

significant difference. Meanwhile, elemental-related Kruskal-Wallis analysis shows that only sediment Zn and Zr/Rb ratios are similar between STM 15-36 and STM 15-31, and other indices between the two specimen sediments are significantly different. For specimen STM 15-36 and the three specimens from DPF, the indices, except the Sr and As contents, are significantly different among this group. In addition, sediment Zr/Rb, Rb/Sr, Nb, and Zn contents are significantly different between DPF and TDYZ.

Discussion

Source of organic matter for the specimen host sediments

Fossils of the Jehol Biota were buried in lacustrine and rarely fluvial sediments (Pan et al., 2013b; Zhou, 2014). These subaqueous sediments, especially lacustrine sediments, receive organic material from both autochthonous (such as lake algae) and allochthonous sources (including grasses, shrubs, and trees that exist on land around lakes and in the shallow parts of lakes as bottom-rooted, emergent vegetation) (Meyers, 1994). Determining the organic matter origins in the host sediment is crucial for the interpretation of the paleoenvironment when the fossil specimen is initially buried.

The sediment C/N ratio has been widely used to distinguish the organic matter source in subaqueous environments (Filippi and Talbot, 2005; Lorente et al., 2014). Fresh organic matter from aquatic algae, which are protein-rich and cellulose-poor, commonly have molar C/N values between 4 and 10, whereas vascular land plants, which are protein-poor and cellulose-rich, usually create organic matter with C/N ratios of 20 and greater (Meyers, 1994). The proportions of sediment organic matter that originate from these two general sources can consequently be distinguished by their characteristic C/N ratios. However, in sediments with low organic matter concentrations (TOC < 0.3%), C/N ratios would be artificially depressed by the unignorable total inorganic nitrogen concentrations, which in turn can lead to misleading interpretations (Meyers, 1997; Meyers, 2003). In this study, the C/N ratios of all the specimen matrices provide

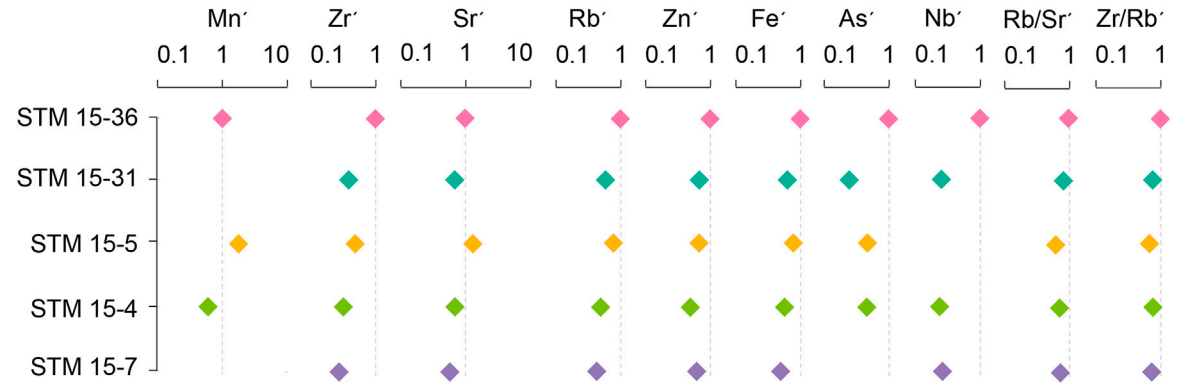

FIGURE 5
Elemental indices standardized according to those of *Sapeornis* STM 15-36's host sediments.

TABLE 3 Kruskal-Wallis analyses of the host sediment indicators between various specimens.

Indices	STM 15-36 vs. 15-31 from TDYZ	STM 15-36 vs. 3 sp.s from DPF	sp.s from DPF vs. from TDYZ
TOC	1	1	0
TN	1	0	0
C/N	1	1	0
$\delta^{13}C_{org}$	1	1	0
Zr	1	1	0
Rb	1	1	0
Sr	1	0	0
Fe	1	1	0
As	1	0	0
Nb	1	1	1
Zn	0	1	1
Zr/Rb	1	1	1
Rb/Sr	0	1	1

"sp." here is the abbreviation of "specimen"; "1" means that the Kruskal-Wallis test rejects the null hypothesis, namely the indicator between those specimens are significantly different, with $p < 0.05$; "0" means the null hypothesis is retained, namely the indicator between those specimens are not significantly different, with $p > 0.05$.

convincing indications of organic sources because all of their TOC significantly exceed 0.3% (Figure 3).

The Kruskal-Wallis analysis shows that the host sediment C/N ratios of STM 15-36 are significantly different from those of the other four specimens (Table 2), implying that the host sediment of STM 15-36 received organic matter from a completely distinct source from the other four. The C/N ratio of the host sediments of STM 15-36 is 24.24 ± 0.79, implying that terrestrial plants provide essentially all of the organic content in the sediment. During the deposition of the host sediment bearing the STM 15-36 fossil, organic materials derived from the terrestrial plants around the lake were brought into the lake by rainfall or rivers, while the lake algae were almost nonexistent. Nonetheless, the C/N ratios of STM 15-31, STM 15-5, STM 15-4, and STM 15-7 are generally lower than 10, falling within the range of aquatic algae. Therefore, *in situ* algae are the dominant organic source for these sediments, and few terrestrial plant materials are transported into the lakes.

Furthermore, the $\delta^{13}C$ of organic matter is always used to support interpretations derived from C/N ratios (Figure 6). Different plants possess various $\delta^{13}C$ values depending on their specific photosynthesis pathways or inorganic carbon sources (Farquhar et al., 1989; Meyers and Ishiwatari, 1993; Cerling et al., 1997; Senut et al., 2009). Terrestrial plants produce organic matter from atmospheric CO_2 ($\delta^{13}C \approx -7‰$); therefore, the $\delta^{13}C$ values of C3 plants generally range from −35‰ to −22‰ with a mean value of approximately −27‰, those of C4 plants are between −10‰ and −15‰ with an average of approximately −14‰, and those of CAM plants range from −10‰ to −22‰ (O'Leary, 1988;

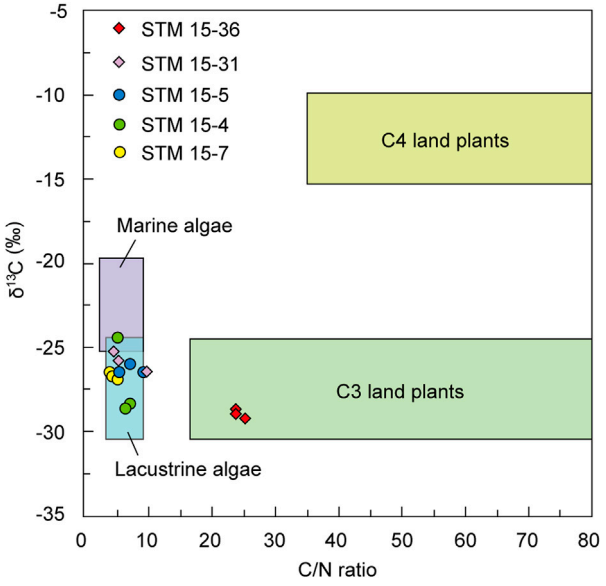

FIGURE 6
$\delta^{13}C_{org}$ and C/N value identifiers for major sources of plant organic matter to subaqueous sediments (Meyers, 1994). Data from Toudaoyingzi are shown as rhombi, and data from Dapingfang are shown as circles.

Farquhar et al., 1989; Cerling et al., 1997; Senut et al., 2009). In addition, the inorganic carbon source for plants in freshwater lakes is dissolved CO_2 ($\delta^{13}C \approx -7‰$), and those plant $\delta^{13}C$ values are distributed between −22‰ and −35‰ (Meyers and Ishiwatari, 1993; Meyers, 1997). Dissolved bicarbonate ($\delta^{13}C \approx 0‰$) in marine or salt lakes is the major carbon source for submerged plants there, resulting in plant $\delta^{13}C$ values of −20‰ to −22‰ (Meyers and Ishiwatari, 1993; Meyers, 1997). The $\delta^{13}C$ characteristics of different plants can be preserved in sediment when the plant residue has been converted into sedimentary organic matter after long-term decomposition (Connin et al., 2001; Liu et al., 2002a; Boström et al., 2007). However, terrestrial C4 plants have occurred considerably since the Middle Miocene (Safe, 2004; Edwards et al., 2010), and CAM plants are usually succulents and mainly distributed in arid regions such as deserts (Senut et al., 2009). Therefore, the influence of terrestrial C4 and CAM plants can be excluded from this study.

The characteristics of the matrix $\delta^{13}C_{org}$ value further identify that the organic matter origin of matrix STM 15-36 is terrestrial C3 plants, while that of the other four is freshwater algae (Figure 6). Therefore, at the initial burial of *Sapeornis* STM 15-36, substantial land plant residuals, accompanied by other land sediments, were transported quickly by river currents or rain washes to the lake, burying the fossil. The Kruskal-Wallis analysis also shows that the matrix $\delta^{13}C_{org}$ value of STM 15-36 is significantly different from those of the other four specimens (Table 2), as they are obviously lower. Two aspects would be attributed to this difference. First, their organic matter derived from different sources possesses various $\delta^{13}C$ values, namely, the $\delta^{13}C$ value of lacustrine algae is generally greater than that of land C3 plants in theory. Second, the contemporaneous climatic factors drove the land plant $\delta^{13}C$ values to be more negative, further influencing the matrix $\delta^{13}C_{org}$ value of STM 15-36. The average $\delta^{13}C$ values of terrestrial C3 plants during the early Aptian were theoretically approximately −26.0‰ (Schubert and Jahren, 2012; Hare et al., 2018). The $\delta^{13}C_{org}$ of the STM15-36 host sediments was approximately −29.03‰, and an approximately 3‰ negative shift in sediment $\delta^{13}C_{org}$ occurred. In the early Aptian, the atmospheric CO_2 content and temperature were considerably higher (Haworth et al., 2005; Sun et al., 2016; Davis, 2017), which are supposed to result in relatively heavier plant $\delta^{13}C$ values (Schleser et al., 1999; Edwards et al., 2000; Wang et al., 2013). However, the high temperature in the early Aptian likely led to greater evaporation at the sea surface, thus creating a wetter global climate, which would result in significantly increased runoff. On the one hand, abundant rainfall affects terrestrial plants' photosynthesis processes, leading to a negative shift in their $\delta^{13}C$ values (Wang and Han, 2001a; Wang and Han, 2001b; Kohn, 2010). On the other hand, strong river currents or rainwash enabled plentiful terrestrial organic matter to be brought into lacustrine sediments. Plentiful rainfall also results in a lake that is too deep to enable aquatic algae to grow due to unsuitable conditions, such as limited sunlight (Farquhar et al., 1982; Gagen et al., 2011). The relatively negative $\delta^{13}C_{org}$ values of the specimen STM 15-36 sediments indicate that paleoprecipitation was abundant and that the paleoenvironment was humid, allowing terrestrial plants to flourish and a large amount of plant debris to be quickly transported to the lake by overland flows.

Paleoclimatic conditions when the specimen was buried

The global climate in the Early Cretaceous was generally warm and interrupted by cold intervals (Larson and Erba, 1999; Grocke et al., 2005; Amiot et al., 2011). However, the contemporaneous climate conditions in the Jehol region and its local area have not been substantially studied (Zhou, 2014). Compared to the global or regional climatic background, paleoclimatic conditions recovered from the specimen host sediments provide a more direct indication of the transportation and preservation of corresponding fossils from the Jehol Biota.

The accumulation of Sr in sediment is usually low under a warm and humid climate, while the deposition of Cu in sediment is hygrophilous (Jin and Li, 2003). Therefore, the sediment Sr/Cu ratio could reflect the paleoclimatic condition, which is a warm-

humid condition when the Sr/Cu ratio ranges from 1 to 10 and a hot-arid environment when it is greater than 10 (Lerman and Baccini, 1978; Liu and Zhou, 2007). The Sr/Cu ratios of the host sediment of STM 15-36 are distributed between 3.05 and 4.01, suggesting that the paleoclimate during the deposition of STM 15-36 was warm and humid. In addition, the sediment Rb/Sr ratio could also effectively reflect the dry-wet conditions due to their distinct response to the weathering effect (Chen et al., 2001; Jin et al., 2001). During weathering, Rb is more stable in the sediment than Sr, as Sr is more likely to leach. As a result, a warm and humid climate would result in an increase in the sediment Rb/Sr ratio, because the abundant rainfall could bring an enhanced weathering effect, which further leads to an increase in Sr loss in the sediment. For sediment Rb/Sr ratios of specimens in this study, those of STM 15-36 are obviously greater than others, especially than those from DPY (Tables 2, 3), suggesting that the paleoclimate for STM 15-36 deposition was warmer and more humid than the other. The Kruskal-Wallis analyses show that the Rb/Sr ratios of sediments from TDYZ are comparable, whereas those from DPF are significantly different from those from TDYZ, indicating that the regional climate of TDYZ possesses better temperature-precipitation conditions than the DPF.

Zr is usually enriched in coarser grains with quartz and feldspar, while Rb usually exists in fine-grained clay minerals (Meng et al., 2000; Dypvik and Harris, 2001); the sediment Zr/Rb ratio thus presents good consistency with the grain size index (Liu et al., 2002b; Chen et al., 2006). In this study, the higher Zr/Rb ratios of the STM 15-36 host sediments (Figure 5) indicate that it contains less clay content than the other four specimens. However, it has been suggested that clay plays an important positive role in soft-tissue preservation in the Jehol Biota (Pan et al., 2013a). There is a conflict in that STM 15-36 presents the most extraordinary preservation of feathers while possessing the coarsest sediment particle size among the five *Sapeornis* specimens. The sediment grain size generally indicates the amount of inflows into the lake and the strength of hydrodynamics (Celina, 1998; Sun et al., 2001) because coarse particles from terrestrial sources are easily deposited under the conditions of plentiful precipitation and intense hydrodynamics. Sediment Sr/Cu and Rb/Sr ratios of specimens have shown that the paleoclimate when *Sapeornis* STM 15-36 was buried is warm and humid. Therefore, a special transportation process such as a rainstorm flush might be partially responsible for the conflict that exists in the preservation of STM 15-36.

A pyroclastic density current from phreatomagmatic eruptions or land surface water was usually attributed to the transportation, during which the entire carcasses of terrestrial Jehol vertebrates survived intact until they reached the lake interior (Jiang et al., 2014). However, fossils formed with pyroclastic flows generally preserve no soft tissues (Xu and Norell, 2004; Evans et al., 2007; Zhao et al., 2007; Xu et al., 2019). The paleoenvironmental analysis of STM 15-36 host sediments shows the occurrence of abundant precipitation and a substantial terrestrial debris input to the host sediments accompanying the transportation of *Sapeornis* STM 15-36. Therefore, the STM 15-36 bird was more likely to be carried by strong land surface flows triggered by the rainstorm into the lake, and was then buried quickly by the accompanying terrestrial debris. This process is more intense and rapid than the transportation of the other four specimens.

But another explanation also could not be excluded by the above evidence, that is *Sapeornis* STM 15-36 was buried in the lake edge while the other four were closer to the lake center, the buried location of STM 15-36 thus received relatively coarser sediments from land.

Deposition environment after the specimen was buried

After the animal is buried, the subaqueous sedimentary environment is critical for the preservation of fossils. Redox-sensitive trace elements (RSEs), mainly including transitional metal elements such as U, Th, Mo, Ni, V, Cr, and Cd, are usually adopted to reflect the redox conditions of paleo-bottom water (Hatch and Leventhal, 1992; Morford and Emerson, 1999; Thomson et al., 2001; Poulichet et al., 2005; Guo et al., 2007; Kentaro and Yasuhiro, 2007). Generally, RSEs share some similar precipitation and enrichment mechanisms in modern marine or lacustrine bottom water. RSE usually exists stably in the bottom water in dissolved states when the water contains normal dissolved oxygen levels. Once the bottom water was in anoxic or anaerobic conditions, the dissolved RSE began to precipitate in the sediments by reduction (Hatch and Leventhal, 1992; Guo et al., 2007). In this study, the sediment contents of RSE, including U, Th, Mo, Ni, and Cu, of STM 15-36 are significantly greater than those of the other four specimens (Figure 4). This result suggests a more oxygen-depleted condition of STM 15-36 with more RSE deposited in the sediment.

In addition, element ratios derived from sediment RSEs can be used to quantify redox conditions (Hatch and Leventhal, 1992; Jones and Manning, 1994; Yan et al., 1998; Kimura and Watanabe, 2001). For example, the geochemical properties of U and Th are similar under reducing conditions but very different under oxidizing conditions (Rogers and Adams, 1976; Wignall and Twitchett, 1996). Therefore, the accumulation of U and Th, which can be reflected by their ratios (U/Th), is different in various redox environments. Generally, an oxygen-rich environment is indicated by a sediment U/Th ratio lower than 0.75, an anoxic environment with a U/Th ratio greater than 1.25, and an oxygen-poor environment with a U/Th ratio of 0.75–1.25 (Hatch and Leventhal, 1992; Wignall and Twitchett, 1996; Kimura and Watanabe, 2001). In this study, only sediment U/Th ratios of

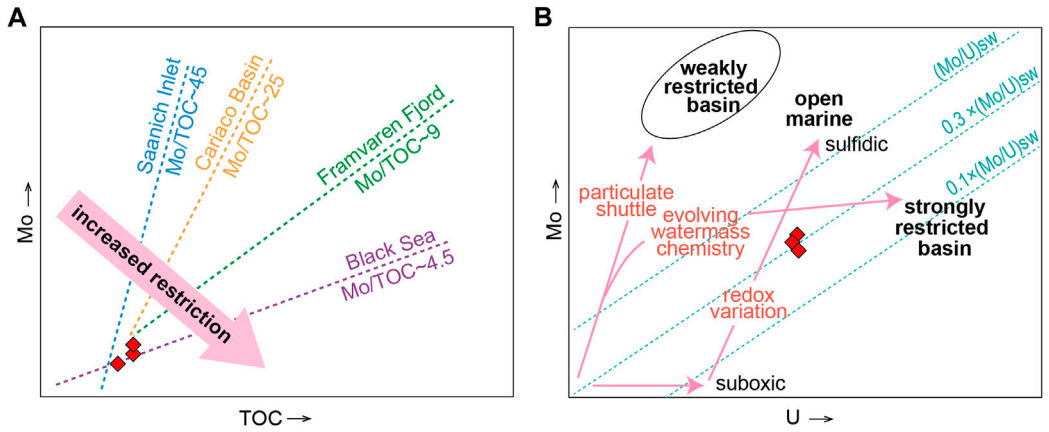

FIGURE 7
Water mass restriction of the sedimentary conditions for specimen STM 15-36, indicated by solid red rhombi in **(A)** Mo versus TOC contents (Algeo and Lyons, 2006) and **(B)** Mo versus U (Algeo and Tribovillard, 2009).

STM 15-36 are available (Table 3), and its high U/Th ratios suggest that the deposition conditions for *Sapeornis* STM 15-36 were almost anoxic.

Furthermore, in ancient low-oxygen water systems, patterns of sediment Mo-TOC and Mo-U covariation can provide information about paleohydrographic conditions, especially the degree of hydrographic restriction of the deepwater mass and temporal changes related to deepwater renewal (Algeo and Lyons, 2006; Algeo and Tribovillard, 2009). Sediment Mo is generally strongly enriched in organic-rich subaqueous facies deposited under oxygen-depleted conditions (Figure 7A). In stagnant basins, the rate of removal of Mo to the sediment generally exceeds the rate of resupply through deepwater renewal, which results in less enrichment of authigenic Mo relative to U and lower Mo/U ratios than seawater (Figure 7B). Among the modern environments, the lowest sediment Mo/TOC ratio is for the Black Sea, followed by Framvaren Fjord, both of which are anoxic silled basins and develop strongly sulfidic environments (Brewer and Spencer, 1974; Skei, 1986; Murray et al., 1989; Dyrssen et al., 1996; Dyrssen, 1999; Algeo and Lyons, 2006). The sediment Mo/TOC ratios of STM 15-36 fall between those of the two above and are relatively closer to those of the Black Sea (Figure 7A), indicating a great restriction of hydrographic conditions as anoxic, stagnant, and strongly sulfidic. This is also supported by the lower sediment Mo/U ratios of STM 15-36 than the seawater ratio of ~7.5–7.9, which indicates a deficiency of aqueous Mo due to the "basin reservoir effect" in a restricted basin (Figure 7B). Therefore, the bottom waters of the paleolake system where *Sapeornis* STM 15-36 is buried are anoxic and restricted.

The Jehol Biota lived in a volcanism-prevalent geological background (Guo and Wang, 2002; Jiang et al., 2011; Pan et al., 2013a; Pan et al., 2013b). Volcanic eruption is one of the important sources of sediment As (Morales-Simfors et al., 2020). The matrix sediments of STM 15-36 contain obviously higher contents of As than those of the other four specimens (Figure 5), implying a greater influence of volcanic activity on the fossilization of *Sapeornis* STM 15-36. Therefore, despite freshwater usually having a low concentration or even absence of sulfate (Pan et al., 2013a), the volcanic activity contributed to a high abundance of sulfur compounds in the freshwater lake (Allison et al., 2008; Zhou, 2014), allowing the sulfidic lacustrine environments for the *Sapeornis* STM 15-36. Therefore, under a quiet, anoxic, and sulfidic depositional environment, microbial activity and bioturbators were inhibited; thus, either the skeleton or feathers of *Sapeornis* STM 15-36 were allowed to be delicately fossilized.

The anoxic, restricted and sulfidic bottom water for *Sapeornis* STM 15-36 usually requires a lake depth that reaches at least the hypolimnion, where is far deeper than the lake edge. So the possibility of a deposition location at the lake edge of STM 15-36 could be ruled out due to this bottom water condition. The relatively coarser grain size of specimen STM 15-36 host sediments mainly resulted from the rapid and strong rainfall into the deep lake. More detailed and accurate understanding of the exceptional preservation of *Sapeornis* STM 15-36 needs to be strengthened by the integration of other technical methods into the research.

Conclusion

Taphonomic analysis of the preservation of the same fossil soft tissues is still lacking. In this study, five specimens of early

bird *S. chaoyangensis* that contained differently preserved feathers were selected. Specimen *Sapeornis* STM 15-36 had a complete set of extraordinarily preserved feathers with a distinct paleoenvironment and preservation conditions. The preliminary conclusion are as follows:

1) The $\delta^{13}C_{org}$ values and C/N ratios of the host sediment indicate that the organic matter of specimen STM 15-36 sediment matrix mainly originated from terrestrial C3 plants, whereas that of specimens STM 15-31, STM 15-5, STM 15-4, and STM 15-7 were mainly derived from lacustrine algae. The obviously lower sediment $\delta^{13}C_{org}$ values of STM 15-36 showed a paleoenvironment with plentiful rainfall.
2) The Sr/Cu and Rb/Sr ratios of the host sediments indicate that the paleoclimate when *Sapeornis* STM 15-36 was buried is warmer and more humid than that of the other four *Sapeornis*. The sediment Zr/Rb ratios suggest that the particle size of the specimen STM 15-36 matrix is the coarsest among the five specimens, conflicting with the most exquisite preservation of its feathers.
3) The redox-sensitive trace elements of host sediments indicate that the bottom waters of the paleolake where *Sapeornis* STM 15-36 was buried are anoxic, restricted, and sulfidic. This deposition environment protected *Sapeornis* STM 15-36 from bioturbation and hydrodynamic disturbance to a large extent, allowing its whole set of feathers to be delicately preserved.
4) We preliminarily propose that a strong and short rain flow brought *Sapeornis* STM 15-36 to lake interior rapidly and then buried it quickly by the accompanying terrestrial debris. With the subsequent anoxic burial environment, a complete set of feathers of *Sapeornis* STM 15-36 was delicately preserved.

Data availability statement

The original contributions presented in the study are included in the article/supplementary material, further inquiries can be directed to the corresponding author.

Author contributions

YZ and X-TZ designed the research, YZ, G-YR, and YG performed the laboratory analysis and collected the data, YZ and QT interpreted the data and prepared the manuscript with contributions from all co-authors.

Funding

This work was co-supported by the National Natural Sciences Foundation of China (Grant Nos 42102007, 41688103, and 42002016), Shandong Provincial Natural Sciences Foundation, China (Grant Nos ZR2018BD013 and ZR2020MD026), and Shandong Provincial Training Program of Innovation and Entrepreneurship for Undergraduates (Grant No. S202210452012).

Acknowledgments

We thank Fucheng Zhang for advice on experimental design and Yibo Yang for valuable discussion. Special thanks to Xuwei Yin and Xiaoli Wang for their assistance in sample collecting.

Conflict of interest

The authors declare that the research was conducted in the absence of any commercial or financial relationships that could be construed as a potential conflict of interest.

Publisher's note

All claims expressed in this article are solely those of the authors and do not necessarily represent those of their affiliated organizations, or those of the publisher, the editors and the reviewers. Any product that may be evaluated in this article, or claim that may be made by its manufacturer, is not guaranteed or endorsed by the publisher.

References

Algeo, T. J., and Lyons, T. W. (2006). Mo-Total organic carbon covariation in modern anoxic marine environments: Implications for analysis of paleoredox and paleohydrographic conditions. *Paleoceanography* 21, PA1016. doi:10.1029/2004pa001112

Algeo, T. J., and Tribovillard, N. (2009). Environmental analysis of paleoceanographic systems based on molybdenum-uranium covariation. *Chem. Geol.* 268 (3–4), 211–225. doi:10.1016/j.chemgeo.2009.09.001

Allison, P. A., Maeda, H., Tuzino, T., and Maeda, Y. (2008)., 23. Japan, 260–266. doi:10.2110/palo.2006.p06-073rExceptional preservation within pleistocene lacustrine sediments of shiobara, Japan*Palaios*

Amiot, R., Wang, X., Zhou, Z., Wang, X. L., Buffetaut, E., Lécuyer, C., et al. (2011). Oxygen isotopes of East Asian dinosaurs reveal exceptionally cold Early Cretaceous climates. *Proc. Natl. Acad. Sci. U. S. A.* 108, 5179–5183. doi:10.1073/pnas.1011369108

Boström, B., Comstedt, D., and Ekblad, A. (2007). Isotope fractionation and ^{13}C enrichment in soil profiles during the decomposition of soil organic matter. *Oecologia* 153 (1), 89–98. doi:10.1007/s00442-007-0700-8

Brewer, P. G., and Spencer, D. W. (1974). Distribution of some trace elements in Black Sea and their flux between dissolved and particulate phases. *Black Sea–Geology, Chem. Biol.* 20, 137–143.

Carvalho, I. S., Novas, F. E., Agnolín, F. L., Isasi, M. P., Freitas, F. I., and Andrade, J. A. (2015b). A Mesozoic bird from Gondwana preserving feathers. *Nat. Commun.* 6 (7141), 7141–7145. doi:10.1038/ncomms8141

Carvalho, I. S., Novas, F. E., Agnolín, F. L., Isasi, M. P., Freitas, F. I., and Andrade, J. A. (2015a). A new genus and species of enantiornithine bird from the early cretaceous of Brazil. *Braz. J. Geol.* 45 (2), 161–171. doi:10.1590/23174889201500020001

Celina, C. (1998). Late Holocene lake sedimentology and climate change in southern Alberta, Canada. *Quat. Res.* 49 (1), 96–101. doi:10.1006/qres.1997.1946

Cerling, T. E., Harris, J. M., Macfadden, J. B., Leakey, M. G., Quade, J., Elsenmann, V., et al. (1997). Global vegetation change through the Miocene/Pliocene boundary. *Nature* 389, 153–158. doi:10.1038/38229

Chang, M., Chen, P. J., Wang, Y., Wang, Y. Q., and Miao, D. (2003). *The Jehol biota: The emergence of feathered dinosaurs, beaked birds, and flowering plants*. Shanghai: Shanghai Scientific & Technical Publishers, 208.

Chen, J., Chen, Y., Liu, L. W., Ji, J. F., Balsam, W., Sun, Y. B., et al. (2006). Zr/Rb ratio in the Chinese loess sequences and its implication for changes in the East Asian winter monsoon strength. *Geochim. Cosmochim. Acta* 70, 1471–1482. doi:10.1016/j.gca.2005.11.029

Chen, J., Wang, Y. J., Chen, Y., Liu, L. W., Ji, J. F., and Lu, H. Y. (2001). Rb and Sr geochemical characterization of the Chinese loess and its implications for palaeomonsoon climate. *Acta Geol. Sin.* 75 (2), 259–266. (in Chinese with English abstract).

Chuong, C. M., Wu, P., Zhang, F. C., Xu, X., Yu, M. K., Widelitz, R. B., et al. (2003). Adaptation to the sky: Defining the feather with integument fossils from mesozoic China and experimental evidence from molecular laboratories. *J. Exp. Zool.* 298, 42–56. doi:10.1002/jez.b.25

Cincotta, A., Nicolaï, M., Campos, H. B. N., McNamara, M., D´Alba, L., Shawkey, M. D., et al. (2022). Pterosaur melanosomes support signalling functions for early feathers. *Nature* 604, 684–688. doi:10.1038/s41586-022-04622-3

Connin, S. L., Feng, X., and Virginia, R. A. (2001). Isotopic discrimination during long-term decomposition in an arid land ecosystem. *Soil Biol. Biochem.* 33 (1), 41–51. doi:10.1016/s0038-0717(00)00113-9

Davis, W. J. (2017). The relationship between atmospheric carbon dioxide concentration and global temperature for the last 425 million years. *Climate* 5 (4), 76. doi:10.3390/cli5040076

Dypvik, H., and Harris, N. B. (2001). Geochemical facies analysis of fine grained siliciclastics using Th/U, Zr/Rb and (Zr+Rb)/Sr ratios. *Chem. Geol.* 181, 131–146. doi:10.1016/s0009-2541(01)00278-9

Dyrssen, D. W. (1999). Framvaren and the Black Sea–similarities and differences. *Aquat. Geochem.* 5, 59–73. doi:10.1023/a:1009663704604

Dyrssen, D. W., Hall, P. O. J., Haraldsson, C., Chierici, M., Skei, J., and Östlund, H. G. (1996). Time dependence of organic matter decay and mixing processes in Framvaren, a permanently anoxic fjord in south Norway. *Aquat. Geochem.* 2, 111–129. doi:10.1007/bf00121627

Edwards, E. J., Osborne, C. P., Strömberg, A. E., Smith, S. A., Bond, W. J., Christin, P. A., et al. (2010). The origins of C4 grasslands: Integrating evolutionary and ecosystem science. *Science* 328, 587–591. doi:10.1126/science.1177216

Edwards, T. W. D., Graf, W., Trimborn, P., Stichler, W., Lipp, J., and Payer, H. D. (2000). $\delta^{13}C$ response surface resolves humidity and temperature signals in trees. *Geochimica Cosmochimica Acta* 64 (2), 161–167. doi:10.1016/s0016-7037(99)00289-6

Evans, S. E., Wang, Y., and Jones, M. E. H. (2007). An aggregation of lizard skeletons from the Lower Cretaceous of China. *Senckenberg. lethaea* 87, 109–118. doi:10.1007/bf03043910

Farquhar, G. D., Ehleringer, J. R., and Hubick, K. T. (1989). Carbon isotope discrimination and photosynthesis. *Annu. Rev. Plant Physiol. Plant Mol. Biol.* 40, 503–537. doi:10.1146/annurev.pp.40.060189.002443

Farquhar, G. D., O´Leary, M. H., and Berry, J. A. (1982). On the relationship between carbon isotope discrimination and the intercellular carbon dioxide concentration in leaves. *Funct. Plant Biol.* 9, 121–137. doi:10.1071/pp9820121

Filippi, M., and Talbot, M. (2005). The palaeolimnology of northern Lake Malawi over the last 25 ka based upon the elemental and stable isotopic composition of sedimentary organic matter. *Quat. Sci. Rev.* 24, 1303–1328. doi:10.1016/j.quascirev.2004.10.009

Foth, C. (2012). On the identification of feather structures in stem-line representatives of birds: Evidence from fossils and actuopalaeontology. *Palaontol. Z.* 86, 91–102. doi:10.1007/s12542-011-0111-3

Gagen, M., Zorita, E., McCarroll, D., Young, G. H. F., Grudd, H., Jalkanen, R., et al. (2011). Cloud response to summer temperatures in Fennoscandia over the last thousand years. *Geophys. Res. Lett.* 38, L05701. doi:10.1029/2010gl046216

Grocke, D. R., Price, G. D., Robinson, S. A., Baraboshkin, E. Y., Mutterlose, J., and Ruffell, A. H. (2005). The Upper Valanginian (Early Cretaceous) positive carbon-isotope event recorded in terrestrial plants. *Earth Planet. Sci. Lett.* 40, 495–509. doi:10.1016/j.epsl.2005.09.001

Gu, Z. W.Nanjing Institute of Geology and Palaeontology; Academia Sinica (1982). "Correlation chart of the Jurassic in China with explanatory text," in *Stratigraphical correlation chart in China with explanatory text* (Beijing: Science Press), 223–240. (in Chinese).

Gu, Z. W. (1962). *Jurassic and cretaceous of China*. Beijing: Science Press, 84. (in Chinese).

Guo, Q. J., Graham, A., Liu, C. Q., Strauss, H., Zhu, M., Pi, D., et al. (2007). Trace element chemostratigraphy of two Ediacaran-Cambrian successions in South China: Implications for organosedimentary metal enrichment and silicification in the early Cambrian. *Palaeogeogr. Palaeoclimatol. Palaeoecol.* 254, 194–216. doi:10.1016/j.palaeo.2007.03.016

Guo, Z. F., Liu, J. Q., and Wang, X. L. (2003). Effect of Mesozoic volcanic eruptions in the Western Liaoning Province, China on paleoclimate and paleoenvironment. *Sci. China (Series D Earth Sci.* 33, 59–71.

Guo, Z. F., and Wang, X. L. (2002). A study on the relationship between volcanic activities and mass mortalities of the Jehol vertebrate fauna from Sihetun, Western Liaoning, China. *Acta Petrol. Sin.* 18, 117–125. (in Chinese with English abstract).

Hare, V. J., Loftus, E., Jeffrey, A., and Ramsey, C. B. (2018). Atmospheric CO_2 effect on stable carbon isotope composition of terrestrial fossil archives. *Nat. Commun.* 9, 252. doi:10.1038/s41467-017-02691-x

Hatch, J. R., and Leventhal, J. S. (1992). Relationship between inferred redox potential of the depositional environment and geochemistry of the Upper Pennsylvanian (Missourian) Stark Shale Member of the Dennis Limestone, Wabaunsee County, Kansas, U.S.A. *Chem. Geol.* 99, 65–82. doi:10.1016/0009-2541(92)90031-y

Haworth, M., Hesselbo, S. P., Mcelwain, J. C., Robinson, S. A., and Brunt, J. W. (2005). Mid-Cretaceous pCO_2 based on stomata of the extinct conifer Pseudofrenelopsis (Cheirolepidiaceae). *Geol.* 33 (9), 749–752. doi:10.1130/g21736.1

He, H. Y., Wang, X. L., Zhou, Z. H., Wang, F., Boven, A., Shi, A., et al. (2004). Timing of the Jiufotang Formation (Jehol Group) in Liaoning, northeastern China, and its implications. *Geophys. Res. Lett.* 31, 1–4. doi:10.1029/2004gl019790

Jiang, B. Y., Fürsich, F. T., and Hethke, M. (2012). Depositional evolution of the Early Cretaceous Sihetun Lake and implications for regional climatic and volcanic history in Western Liaoning, NE China. *Sediment. Geol.* 257-260, 31–44. doi:10.1016/j.sedgeo.2012.02.007

Jiang, B. Y., Fürsichm, F. T., Sha, J. G., Wang, B., and Niu, Y. Z. (2011). Early Cretaceous volcanism and its impact on fossil preservation in Western Liaoning, NE China. *Palaeogeogr. Palaeoclimatol. Palaeoecol.* 302, 255–269. doi:10.1016/j.palaeo.2011.01.016

Jiang, B. Y., Harlow, G. E., Wohletz, K., Zhou, Z. H., and Meng, J. (2014). New evidence suggests pyroclastic flows are responsible for the remarkable preservation of the Jehol biota. *Nat. Commun.* 5, 3151. doi:10.1038/ncomms4151

Jiang, B. Y., and Sha, J. G. (2007). Preliminary analysis of the depositional environments of the Lower Cretaceous Yixian Formation in the Sihetun area, Western Liaoning, China. *Cretac. Res.* 28, 183–193. doi:10.1016/j.cretres.2006.05.010

Jin, M., and Li, W. W. (2003). Petrogeochemical characteristics of Lower Cretaceous and Pliocene rocks and paleoclimate evolution in Wulanhua region. *Uranium Geol.* 19 (6), 349–354. (in Chinese with English abstract).

Jin, Z. D., Wang, S. M., Shen, J., Zhang, E. L., Ji, J. F., and Li, F. C. (2001). Weak chemical weathering during the Little Ice Age recorded by lake sediments. *Sci. China Ser. D-Earth. Sci.* 7, 652–658. doi:10.1007/bf02875338

Jones, B., and Manning, D. A. C. (1994). Comparison of geochemical indices used for the interpretation of palaeoredox conditions in ancient mudstones. *Chem. Geol.* 111, 111–129. doi:10.1016/0009-2541(94)90085-x

Kentaro, M., and Yasuhiro, K. (2007). A new geochemical approach for constraining a marine redox condition of Early Archean. *Earth Planet. Sci. Lett.* 261, 296–302. doi:10.1016/j.epsl.2007.07.020

Kimura, H., and Watanabe, Y. (2001). Oceanic anoxia at the Precambrian-Cambrian boundary. *Geol.* 29 (11), 995–998. doi:10.1130/0091-7613(2001)029<0995:oaatpc>2.0.co;2

Kohn, M. J. (2010). Carbon isotope compositions of terrestrial C3 plants as indicators of (paleo)ecology and (paleo)climate. *Proc. Natl. Acad. Sci. U. S. A.* 107 (46), 19691–19695. doi:10.1073/pnas.1004933107

Larson, R. L., and Erba, E. (1999). Onset of the mid-Cretaceous greenhouse in the Barremian-Aptian: igneous events and the biological, sedimentary, and geochemical responses. *Paleoceanography* 14, 663–678. doi:10.1029/1999pa900040

Lerman, A., and Baccini, P. (1978). Lakes-Chemistry, Geology, Physics. *J. Geol.* 88 (2), 249–250.

Liu, G., and Zhou, D. S. (2007). Application of microelements analysis in identifying sedimentary environment- taking Qianjiang Formation in the Jianghan Basin as an example. *Petroleum Geol. Exp.* 29 (3), 307–310. (in Chinese with English abstract).

Liu, L. W., Chen, J., Chen, Y., Ji, J. F., and Lu, H. Y. (2002a). Variation of Zr/Rb values in loess since the last 130 ka and its implication for winter monsoon. *Chin. Sci. Bull.* 47 (9), 702–706. (in Chinese with English abstract).

Liu, W. G., Ning, Y. F., An, Z. S., Wu, Z. H., Lu, H. Y., and Cao, Y. N. (2002b). The response to vegetation of modern soil and paleosol organic carbon isotope in Loess Plateau. *Sci. China (Series D Earth Sci.* 32 (10), 830–836.

Lorente, F. L., Pessenda, L. C., Oboh-Ikuenobe, F., Biso, A. A., Cohen, M., Meyer, K. E. B., et al. (2014). Palynofacies and stable C and N isotopes of Holocene sediments from Lake Macuco (Linhares, Espírito Santo, southeastern Brazil): Depositional settings and palaeoenvironmental evolution. *Palaeogeogr. Palaeoclimatol. Palaeoecol.* 415, 69–82. doi:10.1016/j.palaeo.2013.12.004

McNamara, M. E., Zhang, F. C., Kearns, S. L., Orr, P. J., Toulouse, A. F., Tara, H., et al. (2018). Fossilized skin reveals coevolution with feathers and metabolism in feathered dinosaurs and early birds. *Nat. Commun.* 9, 2072. doi:10.1038/s41467-018-04443-x

Meng, X. W., Du, D. W., Chen, Z. H., and Wang, X. Q. (2000). Factors controlling spatial variation of $^{87}Sr/^{86}Sr$ in the fine-grained sediments from the overbanks of the Yellow River and Yangtze River and its implication for provenance of marine sediments. *Geochimica* 29 (6), 562–570. (in Chinese with English abstract).

Meyers, P. A. (2003). Applications of organic geochemistry to paleolimnological reconstructions: a summary of examples from the Laurentian Great Lakes. *Org. Geochem.* 34, 261–289. doi:10.1016/s0146-6380(02)00168-7

Meyers, P. A., and Ishiwatari, R. (1993). Lacustrine organic geochemistry – an overview of indicators of organic matter sources and diagenesis in lake sediments. *Org. Geochem.* 20 (7), 867–900. doi:10.1016/0146-6380(93)90100-p

Meyers, P. A. (1997). Organic geochemical proxies of paleoceanographic, paleolimnologic, and paleoclimatic processes. *Org. Geochem.* 27 (5/6), 213–250. doi:10.1016/s0146-6380(97)00049-1

Meyers, P. A. (1994). Preservation of elemental and isotopic source identification of sedimentary organic matter. *Chem. Geol.* 27 (5), 289–302. doi:10.1016/0009-2541(94)90059-0

Morales-Simfors, N., Bundschuh, J., Herath, I., Inguaggiato, C., Caselli, A. T., Tapia, J., et al. (2020). Arsenic in Latin America: A critical overview on the geochemistry of arsenic originating from geothermal features and volcanic emissions for solving its environmental consequences. *Sci. Total Environ.* 716, 135564. doi:10.1016/j.scitotenv.2019.135564

Morford, J. L., and Emerson, S. (1999). The geochemistry of redox sensitive trace metals in sediments. *Geochimica CosMochimica Acta* 63 (11–12), 1735–1750. doi:10.1016/s0016-7037(99)00126-x

Murray, J. W., Jannasch, H. W., Honjo, S., Anderson, R. F., Reeburgh, W. S., Top, Z., et al. (1989). Unexpected changes in the oxic/anoxic interface in the Black Sea. *Nature* 338, 411–413. doi:10.1038/338411a0

O'Connor, J. K., Chiappe, L. M., Chuong, C. M., Bottjer, D. J., and You, H. L. (2012). Homology and potential cellular and molecular mechanisms for the development of unique feather morphologies in early birds. *Geosciences* 2, 157–177. doi:10.3390/geosciences2030157

O'Leary, M. H. (1988). Carbon isotopes in photosynthesis: Fractionation techniques may reveal new aspects of carbon dynamics in plants. *BioScience* 38 (5), 328–336. doi:10.2307/1310735

Pan, Y. H., Sha, J. G., and Fürsich, F. T. (2013a). A model for organic fossilization of the Early Cretaceous Jehol lagerstätte based on the study of the taphonomy of 'Ephemeropsis trisetalis. *Palaios* 29 (7), 363–377. doi:10.2110/palo.2013.119

Pan, Y. H., Sha, J. G., and Yao, X. G. (2012). Taphonomy of Early Cretaceous freshwater bivalve concentrations from the Sihetun area, Western Liaoning, NE China. *Cretac. Res.* 34, 94–106. doi:10.1016/j.cretres.2011.10.007

Pan, Y. H., Sha, J. G., Zhou, Z. H., and Fürsich, F. T. (2013b). The Jehol Biota: definition and distribution of exceptionally preserved relicts of a continental Early Cretaceous ecosystem. *Cretac. Res.* 44, 30–38. doi:10.1016/j.cretres.2013.03.007

Pan, Y. H., Zheng, W. X., Moyer, A. E., O'Connor, J. K., Wang, M., Zheng, X. T., et al. (2016). Molecular evidence of keratin and melanosomes in feathers of the Early Cretaceous bird Eoconfuciusornis. *Proc. Natl. Acad. Sci. U. S. A.* 113 (49), E7900–E7907. doi:10.1073/pnas.1617168113

Pan, Y. H., Zheng, W. X., Sawyer, R. H., Pennington, M. W., Zheng, X. T., Wang, X. L., et al. (2019). The molecular evolution of feathers with direct evidence from fossils. *Proc. Natl. Acad. Sci. U. S. A.* 116 (8), 3018–3023. doi:10.1073/pnas.1815703116

Poulichet, F. E., Seidel, J. L., Jezequel, D., Metzger, E., Prevot, F., Simonucci, C., et al. (2005). Sedimentary record of redox-sensitive elements (U, Mn, Mo) in a transitory anoxic basin (the Thau lagoon, France). *Mar. Chem.* 95 (3–4), 271–281. doi:10.1016/j.marchem.2004.10.001

Provini, P., Zhou, Z. H., and Zhang, F. C. (2009). "A new species of the basal bird *Sapeornis* from the early cretaceous of Liaoning, China," in *Vertebrae PalAsiatica* 47, 194–207.

Rogers, J. J. W., and Adams, J. A. S. (1976). *Handbook of thorium and uranium geochemistry*. Beijing: Atomic Press, 1–106. (in Chinese).

Safe, R. F. (2004). The evolution of C4 photosynthesis. *New Phytol.* 61, 341–370. doi:10.1111/j.1469-8137.2004.00974.x

Schleser, G. H., Helle, G., Lücke, A., and Vos, H. (1999). Isotope signals as climate proxies: the role of transfer functions in the study of terrestrial archives. *Quat. Sci. Rev.* 18, 927–943. doi:10.1016/s0277-3791(99)00006-2

Schubert, B. A., and Jahren, A. H. (2012). The effect of atmospheric CO_2 concentration on carbon isotope fractionation in C3 land plants. *Geochim. Cosmochim. Acta* 96, 29–43. doi:10.1016/j.gca.2012.08.003

Senut, B., Pickford, M., and Se ´galen, L. (2009). Neogene desertification of Africa. *Comptes Rendus Geosci.* 341 (8–9), 591–602. doi:10.1016/j.crte.2009.03.008

Serrano, F. J., Pittman, M., Kaye, T. G., Wang, X. L., Zheng, X. T., and Chiappe, L. M. (2020). Laser-Stimulated Fluorescence refines flight modelling of the Early Cretaceous bird Sapeornis. *Bull. Am. Mus. Nat. Hist.* 4TK, 333–344.

Sha, J. G. (2007). Cretaceous stratigraphy of northeast China: non-marine and marine correlation. *Cretac. Res.* 28, 146–170. doi:10.1016/j.cretres.2006.12.002

Skei, J. (1986). The biogeochemistry of Framvaren: A permanent anoxic fjord near Farsund. *Rep. Nor. Inst. Vannforsk.* 67, 603. doi:10.1029/EO067i031p00603-02

Sun, Q. L., Zhou, J., and Xiao, J. L. (2001). Grain-size characteristics of lake Daihai sediments and its palaeoenvironment significance. *Mar. Geol. Quat. Geol.* 21 (1), 93–95. (in Chinese with English abstract).

Sun, Y. W., Li, X., Zhao, G. W., Liu, H., and Zhang, Y, L. (2016). Aptian and Albian atmospheric CO_2 changes during oceanic anoxic events: Evidence from fossil Ginkgo cuticles in Jilin Province, Northeast China. *Cretac. Res.* 62, 130–141. doi:10.1016/j.cretres.2015.12.007

Thomson, J., Nixon, S., Croudace, I. W., Pedersen, T. F., Brown, L., Cook, G. T., et al. (2001). Redox-sensitive element uptake in north-east Atlantic Ocean sediments (Benthic Boundary Layer Experiment sites). *Earth Planet. Sci. Lett.* 184 (2), 535–547. doi:10.1016/s0012-821x(00)00347-2

Ullmann, P. V., Grandstaff, D. E., Ash, R. D., and Lacovara, K. J. (2020). Geochemical taphonomy of the Standing Rock Hadrosaur Site: Exploring links between rare Earth elements and cellular and soft tissue preservation. *Geochimica Cosmochimica Acta* 269, 223–237. doi:10.1016/j.gca.2019.10.030

Wang, G. A., and Han, J. M. (2001b). $\delta^{13}C$ variations of C3 plants in dry and rainy seasons. *Mar. Geol. Quat. Geol.* 21 (4), 43–47. (in Chinese with English abstract).

Wang, G. A., and Han, J. M. (2001a). Relations between $\delta^{13}C$ values of C3 plant in northwestern China and annual precipitation. *Chin. J. Geol.* 36 (4), 494–499. (in Chinese with English abstract).

Wang, G. A., Li, J. Z., Liu, X. Z., and Li, X. Y. (2013). Variations in carbon isotope ratios of plants across a temperature gradient along the 400 mm isoline of mean annual precipitation in north China and their relevance to paleovegetation reconstruction. *Quat. Sci. Rev.* 63, 83–90. doi:10.1016/j.quascirev.2012.12.004

Wang, X. L., O'Connor, J. K., Maina, J. N., Pan, Y. H., Wang, M., Wang, Y., et al. (2018). Archaeorhynchus preserving significant soft tissue including probable fossilized lungs. *Proc. Natl. Acad. Sci. U. S. A.* 115, 11555–11560. doi:10.1073/pnas.1805803115

Wang, X. L., O'ConnorZheng, X. T., Wang, M., Hu, H., and Zhou, Z. H. (2014). Insights into the evolution of rachis dominated tail feathers from a new basal enantiornithine (Aves: Ornithothoraces). *Biol. J. Linn. Soc. Lond.* 113, 805–819. doi:10.1111/bij.12313

Wang, X. L., Pittman, M., Zheng, X. T., Kaye, T. G., Falk, A., Hartman, S., et al. (2017a). Basal paravian functional anatomy illuminated by high-detail body outline. *Nat. Commun.* 8 (1), 14576. doi:10.1038/ncomms14576

Wang, X. L., Wang, Y. Q., Xu, X., Wang, Y., Zhang, J. Y., Zhang, F. C., et al. (1999). Record of the Sihetun vertebrate mass mortality events Western Liaoning, China: Caused by volcanic eruptions. *Geol. Rev.* 45, 458–467.

Wang, X. L., and Zhou, Z. H. (2003). "Mesozoic Pompeii," in *The Jehol biota*. Editor M. M. Chang (Shanghai: Shanghai Scientific and Technical Publlishers), 19–36.

Wang, Y., Hu, H., O'Connor, J. K., Wang, M., Xu, X., Zhou, Z. H., et al. (2017b). A previously undescribed specimen reveals new information on the dentition of *Sapeornis chaoyangensis*. *Cretac. Res.* 74, 1–10. doi:10.1016/j.cretres.2016.12.012

Wang, Y., Wang, M., O'Connor, J. K., Wang, X. L., Zheng, X. T., and Zhang, X. M. (2016). A new Jehol enantiornithine bird with three-dimensional preservation and ovarian follicles. *J. Vertebrate Paleontology* 36 (2), e1054496. doi:10.1080/02724634.2015.1054496

Wignall, P. B., and Twitchett, R. J. (1996). Oceanic anoxia and the end Permian mass extinction. *Science* 272, 1155–1158. doi:10.1126/science.272.5265.1155

Xu, X., and Norell, M. A. (2004). A new troodontid dinosaur from China with avian-like sleeping posture. *Nature* 431, 838–841. doi:10.1038/nature02898

Xu, X., Zhou, Z. H., Wang, Y., and Wang, M. (2019). Study on Jehol Biota: recent advances and future prospects. *Sci. China Earth Sci.* 49, 1491–1511.

Yan, J. X., Xu, S. P., and Li, F. L. (1998). Geochemistry of the dysaerobic sedimentary environments of the Qixia Formation in Badong, Hubei. *Sediment. Facies Palaeogeogr.* 18 (6), 27–32. (in Chinese with English abstract).

Yang, W., Li, S., and Jiang, B. (2007). New evidence for Cretaceous age of the feathered dinosaurs of Liaoning: zircon U-Pb SHRIMP dating of the Yixian Formation in Sihetun, northeast China. *Cretac. Res.* 28, 177–182. doi:10.1016/j.cretres.2006.05.011

Zhang, F. C., Kearns, S. L., Orr, P. J., Benton, M. J., Johnson, D., Xu, X., et al. (2010). Fossilized melanosomes and the colour of Cretaceous dinosaurs and birds. *Nature* 463, 1075–1078. doi:10.1038/nature08740

Zhang, F. C., Zhou, Z. H., and Dyke, G. (2006). Feathers and 'feather-like' integumentary structures in Liaoning birds and dinosaurs. *Geol. J.* 41, 395–404. doi:10.1002/gj.1057

Zhang, F. C., and Zhou, Z. H. (2004). Leg feathers in an Early Cretaceous bird. *Nature* 431, 925. doi:10.1038/431925a

Zhao, Q., Barrett, P. M., and Eberth, D. A. (2007). Social behaviour and mass mortality in the basal ceratopsian dinosaur Psittacosaurus (Early Cretaceous, People's Republic of China). *Palaeontology* 50, 1023–1029. doi:10.1111/j.1475-4983.2007.00709.x

Zheng, X. T. (2009). *Avian origin*. Jinan: Shandong Science and Technology Press, 51. (in Chinese).

Zheng, X. T., O'Connor, J. K., Wang, X. L., Pan, Y. H., Wang, Y., Wang, M., et al. (2017). Exceptional preservation of soft tissue in a new specimen of *Eoconfuciusornis* and its biological implications. *Natl. Sci. Rev.* 4, 441–452. doi:10.1093/nsr/nwx004

Zheng, X. T., O'Connor, J. K., Wang, X. L., Wang, M., Zhang, X. M., and Zhou, Z. H. (2014). On the absence of sternal elements in *Anchiornis* (Paraves) and *Sapeornis* (Aves) and the complex early evolution of the avian sternum. *Proc. Natl. Acad. Sci. U. S. A.* 111, 13900–13905. doi:10.1073/pnas.1411070111

Zhou, Z. G., and Zhang, F. C. (2003). Anatomy of the primitive bird *Sapeornis chaoyangensis* from the Early Cretaceous of Liaoning, China. *Can. J. Earth Sci.* 40, 731–747. doi:10.1139/e03-011

Zhou, Z. H., Barrett, P. M., and Hilton, J. (2003). An exceptionally preserved Lower Cretaceous ecosystem. *Nature* 421, 807–814. doi:10.1038/nature01420

Zhou, Z. H., Meng, Q. R., Zhu, R. X., and Wang, M. (2021). Spatiotemporal evolution of the Jehol Biota: Responses to the North China craton destruction in the Early Cretaceous. *Proc. Natl. Acad. Sci. U. S. A.* 118 (34), e2107859118. doi:10.1073/pnas.2107859118

Zhou, Z. H. (2014). The Jehol Biota, an Early Cretaceous terrestrial Lagerstätte: new discoveries and implications. *Natl. Sci. Rev.* 1, 543–559. doi:10.1093/nsr/nwu055

Zhou, Z. H., and Zhang, F. C. (2002). Largest bird from the Early Cretaceous and its implications for the earliest avian ecological diversification. *Naturwissenschaften* 89, 34–38. doi:10.1007/s00114-001-0276-9

Zhu, R. X., Shao, J. A., Pan, Y. X., Shi, R. P., Shi, G. H., and Li, D. M. (2001). Paleomagnetic data from Early Cretaceous volcanic rocks of west Liaoning: Evidence for intracontinental rotation. *Chin. Sci. Bull.* 47, 1832–1837. doi:10.1360/02tb9400

Zhu, Y. H., and He, C. Q. (2007). Middle Jurassic to Early Cretaceous dinoflagellate assemblage zones in eastern Heilongjiang Province, northeast China. *Cretac. Res.* 28, 327–332. doi:10.1016/j.cretres.2006.10.001

Zhu, Y. H., and He, C. Q. (2003). The Middle Jurassic to Early Cretaceous dinoflagellate assemblage sequence from eastern Heilongjiang. *J. Stratigr.* 27, 282–288. (in Chinese with English abstract).